A Novel Efficient Ray-Tracing Method for Designing Non-Resonant Partially Reflective Surface Antennas

(Article begins on next page)

A Novel Efficient Ray-Tracing Method for Designing Non-Resonant Partially Reflective Surface Antennas

Xiaodong Zheng(1), Yuehe Ge(1), Ladislau Matekovits(2), and Zhizhang (David) Chen(3), (1)

(1) Fuzhou University, Fuzhou, Fujian, China (yuehe@ieee.org)
(2) Politecnico di Torino, Torino, Italy (ladislau.matekovits@polito.it)
(3) Dalhousie University, Halifax, Canada (zz.chen@ieee.org)

***Abstract*—Recently, non-resonant partially-reflective surface (PRS) antennas have emerged as promising alternatives to conventional PRS antennas. However, the design of non-resonant PRS antennas is somewhat complicated. In this paper, we introduce a straightforward ray-tracing method aimed at efficiently calculating the necessary compensation phases. Through simulations conducted using Ansys HFSS, the effectiveness of our proposed method is demonstrated.**

I. Introduction

Since the introduction of the electromagnetic (EM) bandgap concept, there has been extensive research on partially reflecting surface (PRS) resonant antennas [1], [2], also known as Fabry-Perot resonator antennas [3]. While they offer high-gain performance and advantages such as a simple structure, easy assembly, and low cost, their gain levels are somewhat constrained. Recently, a novel non-resonant PRS antenna concept has been introduced [4], promising enhanced design flexibility and superior gain performance. However, the design of non-resonant PRS antennas requires consideration of the near fields on the PRS surface [4], necessitating the utilization of 3D electromagnetic simulation software.

This paper introduces a pioneering approach for the efficient design of non-resonant PRS antennas. Leveraging a modified ray-tracing method inspired by techniques previously employed in the design of PRS resonant antennas [1], our novel methodology enables the approximate calculation of the phase distribution within the near fields on the PRS. Consequently, this facilitates the determination of the necessary compensation phases and the subsequent design of a phase-correcting surface (PCS). The effectiveness of our proposed method is validated through simulations conducted using Ansys HFSS.

II. Theoretical analysis

Figure 1 illustrates the 2-D schematic diagram of a typical non-resonant PRS antenna [4], which comprises a feeding antenna, a fully reflective ground (GND), a PRS, and a PCS. Upon transmission from the feeding antenna, EM waves undergo partial transmission and reflection by the PRS. In cases where the cavity is not resonant at the operating frequency, the transmitted EM waves tend to be out-of-phase on the surface of the PRS. To address this, the PCS facilitates full transmission of incoming EM waves and provides the necessary compensation phases. This ensures that the EM waves on the top surface of the PCS become in-phase, generating a focused high-gain beam directed broadside to the PRS antenna.

The PRS and PCS under consideration are characterized by their periodic structures, as illustrated in Fig. 1, where various unit cells are depicted with distinct colors. These colors signify potential variations in reflection coefficients or the provision of different compensation phases. Employing the Huygens principle [5], the periodic nature of the PRS and PCS allows them to be treated as secondary radiation sources, essentially forming antenna arrays. Consequently, our analysis focuses on EM waves that either pass through or are radiated by individual unit cells. For efficient consideration, the EM waves are assumed to pass through the center of each unit cell. Given that the reflection phase of the GND is π, the phase angle of the *n*-th leaky wave, pertaining to the *n*-th unit cell on the PRS, can be expressed as follows:

$$\theta_n = \mathrm{n}\left(-\frac{2\pi}{\lambda}\frac{2h}{\cos\alpha} - \pi\right) + \sum_{i=1}^{n}\varphi_i + \theta_0 \qquad (1)$$

where α is the angle determined by the center of the unit cell, as shown in Fig. 1, φ_i and θ_0 are reflection phase of the *i*-th unit cell on the PRS and the reference phase, respectively. The PCS is constructed according to the compensated phases based on Eq. (1). Consequently, these compensation phases can be calculated using Formula (1) rather than relying on 3-D electromagnetic (EM) software, resulting in significant computational time savings and streamlining the antenna design process.

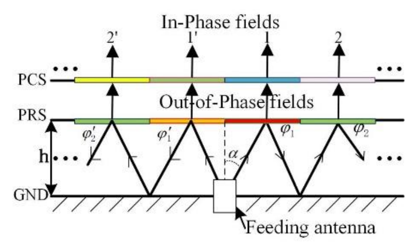

Figure 1. Schematic of a non-resonant PRS antenna.

III. Validation

This section presents the design and validation of a non-resonant PRS antenna operating at 12.5 GHz, aiming to confirm the efficacy of the previously outlined design strategy. Illustrated in Fig. 2 is the configured PRS antenna (referred to as Ant. 1), comprising a metal ground, a PRS, a PCS, and a compact open waveguide feed antenna. Both the PRS and PCS are constructed as Fabry-Perot metasurfaces [6], sharing the same period and providing partial reflection and compensation phases, respectively. In this specific design, the cavity height (h1) is set at 0.625λ, and there exists a 3 mm gap (h2) between the PRS and the PCS. Employing Formula (1), the phase distribution on the centers of all unit cells of the PRS is calculated. Subsequently, 3-bit phases, comprising 8 phases with a uniform step of 45°, are used to compensate these phases through the PCS. The resulting compensation phase distribution on the PCS is then obtained and visualized in Fig. 2(b).

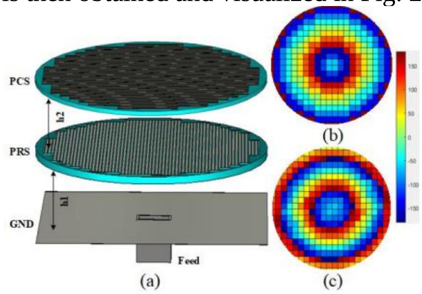

Figure 2. (a) The designed PRS antenna; (b) The compensation phase distribution from Formula (1); (c) The compensation phase distribution from Ansys HFSS.

To validate the design, we utilize an open waveguide as the feed. The PRS and PCS feature two identical dielectric cells and three metal layers. The top and bottom metal layers consist of orthogonally-oriented gratings, while the middle layer adopts a double splitting ring (DSR) structure, as depicted in Fig. 3. The required transmission compensation phases for the PCS are obtained by adjusting the parameters of the DSR [6]. Figure 3 illustrates the transmission amplitudes and phases for eight distinct PCS unit cells. Notably, the transmission efficiency exceeds 95%, and there is a consistent 45° phase step among the eight cells at 12.5 GHz. One of these eight cells is selected to construct the PRS, and by rotating the DSR, the necessary partial reflection is achieved [6].

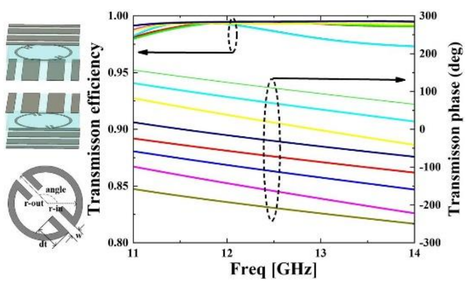

Figure 3. Transmission amplitudes and phases of the basic eight units of the PCS.

Utilizing the aforementioned design, we employ the eight unit cells to construct both the PRS and PCS. Subsequently, we have created the HFSS model for the PRS antenna and conduct comprehensive simulations. For comparative analysis, we also design a distinct PRS antenna denoted as Ant. 2. In this scenario, the antenna configuration mirrors that of Ant. 1, while the compensation phases are determined by recording the near fields at the central position of each unit cell beneath the PRS using Ansys HFSS. The resulting compensation phase pattern is visualized in Fig. 2(c), guiding the design of a separate PCS tailored specifically for Ant. 2.

Simulations were conducted for both Ant. 1 and 2, and the comparative results are depicted in Fig. 4. Both ray-tracing and HFSS-based designs yield the anticipated pencil beam. While the peak gain achieved through ray-tracing compensation closely aligns with that obtained through HFSS, there is a marginal reduction in peak gain at nearby frequency points. Specifically, the peak gain reaches 20.1 dBi using the proposed efficient method. The 3-dB gain bandwidth is measured at 12%, with the aperture efficiency standing at approximately 30.47%. These findings highlight the effectiveness of the proposed ray-tracing approach in achieving the desired antenna performance, showcasing comparable results to traditional EM software-based PRS antennas.

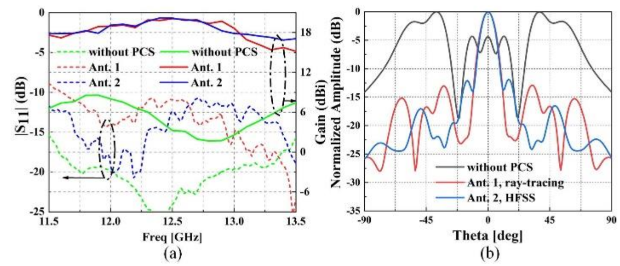

Figure 4. Simulation results for PRS antennas without PCS and with the PCS designed by the proposed ray-tracing method or Ansys HFSS: (a) Realized gain and $|S_{11}|$; (b) Radiation patterns.

IV. Conclusion

We introduce a straightforward ray-tracing method for the efficient design of non-resonant partially reflective surface antennas. Simulation results reveal that, in comparison to the accurate yet complex design approach, the outcomes from our proposed simple, efficient method are comparable, affirming its effectiveness in achieving reliable results with reduced design intricacy.

Acknowledgment

This research was supported by the National Natural Science Foundation of China (NSFC) (62071187, 62071125), the Industry-Education Cooperation Project in Fujian Province, China (2022H6018), and Fujian Province Major Special Topic Project (2022HZ026007).

References

[1] G. von Trentini, “Partially reflecting sheet arrays,” *IEEE Trans. Antennas Propag.*, vol. 4, pp. 666–671, Oct. 1956.

[2] P. Xie, G. Wang, and X. Zou, ”Gain and AR Improvements of the Wideband Circularly Polarized Fabry-Perot Resonator Antenna,” *IEEE Trans. Antennas Propag.*, vol. 69, no. 10, pp. 6965-6970, Oct. 2021.

[3] A. Lalbakhsh, M. U. Afzal, K. P. Esselle, and S. L. Smith, “Wideband near-field correction of a Fabry–Pérot resonator antenna,” *IEEE Trans. Antennas Propag.*, vol. 67, no. 3, pp. 1975–1980, Mar. 2019.

[4] X. Ren, Y. Ge, and Z. D. Chen, ”A Partially Reflecting Surface Antenna With a Non-Resonant Cavity and a Phase-Correcting Surface for Gain Enhancement,” *IEEE Trans. Antennas Propag.*, vol. 71, no. 2, pp. 1244-1253, Feb. 2023.

[5] S. Lin, Y. Ge, *et al*., “On the Use of a Metasurface Lens Over a Large-Element-Spacing Antenna Array for Grating-Lobe Suppression and Gain Enhancement,” *TechRxiv. Preprint.* https://doi.org/10.36227/techrxiv.21813942.v1.

[6] Y. Wang, Y. Ge, *et al*., ”Broadband High-Efficiency Ultrathin Metasurfaces With Simultaneous Independent Control of Transmission and Reflection Amplitudes and Phases,” *IEEE Trans Microw Theory* Tech., vol. 70, no. 1, pp. 254-263, Jan. 2022.